Improvement of thermal management of composites forming tools using lattice structures

Matthis Balthazar, Nicolas Baudin, Jérôme Soto, Sébastien Guéroult, Vincent Sobotka

Improvement of thermal management of composites forming tools using lattice structures

Matthis Balthazar[1,2,a], Nicolas Baudin[2,b], Jérôme Soto[2,3,c], Sébastien Guéroult[1,d], Vincent Sobotka[2,e*]

[1] Institut de Recherche Technologique Jules Verne, 1 Mail des 20 000 Lieues, Bouguenais, 44340, France

[2] Nantes Université, CNRS, Laboratoire de thermique et énergie de Nantes, LTeN, UMR 6607, La Chantrerie, rue Christian Pauc, Nantes, 44306 cedex 03, France

[3] Icam school of engineering, Nantes Campus, 35 avenue du champ de manœuvres, Carquefou, 44470, France

[1, 2]matthis.balthazar@univ-nantes.fr, [2]nicolas.baudin@univ-nantes.fr, [2, 3]jerome.soto@icam.fr, [1]sebastien.gueroult@irt-jules-verne.fr, [2]vincent.sobotka@univ-nantes.fr (*corresponding author)

Keywords: Composite manufacturing, Lattice structure, Thermal management, Tooling

Abstract. The manufacture of composite parts is a complex process, where the final quality of the part depends on several parameters, one of which is crucial: thermal management during the manufacturing process. Whatever the process, thermal management must be carried out with accuracy. Traditional management with circular channels, whether optimized or not, has its limits in terms of efficiency and temperature uniformity, particularly for complex geometries. To overcome these limitations, the use of porous media, and lattice structures in particular, is an alternative for improving uniformity and efficiency. This system, in which the cooling fluid circulates in the lattice structure, is studied in this work in order to analyze heat transfer and fluid dynamics locally, and to demonstrate the feasibility of the system.

Introduction

Composite parts are widely used in industry thanks to their advantageous properties, but the manufacturing process must be precisely controlled, especially thermal management. In fact, it is responsible for the final quality of the part, the productivity of the process and its energy consumption. Three factors are important in temperature management: the temperature levels [1, 2], the cooling rate [3, 4] and the temperature field uniformity [5]. In terms of productivity, for thermo-stamping process, the time dedicated to part cooling can account for more than half the cycle time [6]. Improving thermal management efficiency is therefore important to improve the final quality of parts and process productivity. As convective heat transfer enables supply and release of heat using the same cooling fluid, this mode is traditionally used in tooling design. In this case, the fluid flows inside straight channels or channels that follow the shape of the part for the conformal cooling. Although the improvement brought about by conformal channels is proven [7], even optimized channels are limited in location by design rules. The distance between the channel and the tooling surface (d_2 in Fig. 1) should generally be at least one channel diameter (d_c in Fig. 1), to avoid thermal marking. This distance is responsible for the thermal inertia of the tooling, which impacts the thermal response time of the tooling and the energy consumption of the process. To reduce the distance between the fluid and the tooling surface and avoid the phenomenon of thermal marking, the use of a porous medium in which the heat transfer circulates is considered in this study here, as shown in Fig. 1. The porous medium creates a sheet-like flow,

allowing a constant distance between the fluid and the tool surface, avoiding thermal marking, and offers structural reinforcement, providing mechanical strength. The porous medium studied here is a lattice structure, thanks to its great performance in terms of thermal efficiency [8] and mechanical strength [9].

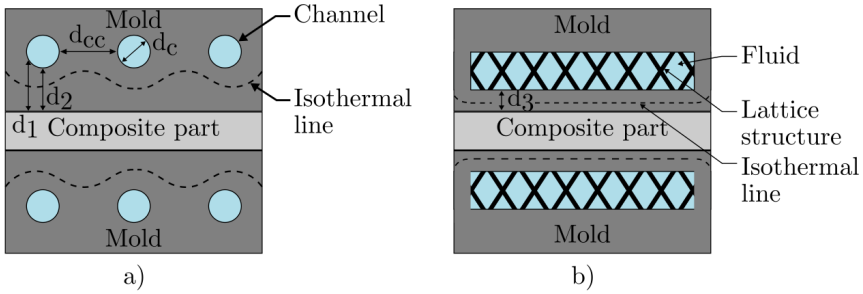

Figure 1: Schematic representation of a) conventional channels b) system studied in this work

The aim of this article is to numerically analyze local heat transfer and fluid flow as a function of the fluid used, oil or water, and to develop an experimental bench to validate the feasibility and efficiency of lattice structures.

Method

Numerical method.

The aim of the numerical simulations is to analyze local heat transfer and fluid flow phenomena, considering steady-state flow. The numerical domain of the study is reduced in relation to the overall tooling, due to the numerical cost implied by its size.

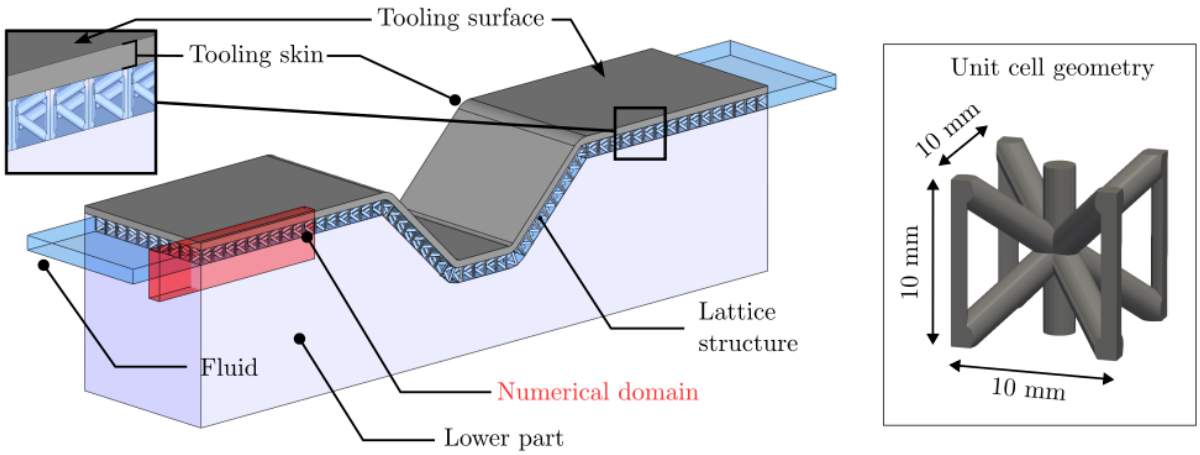

Figure 2: concept of the tooling and numerically studied area

Thermal and fluidic phenomena are analyzed on a section of the tooling; the area studied is shown in red in Figure 2. The lattice structure geometry used is a cubic-centered BCC geometry with additional spacers, referred to here as BCCZ+. The advantage of this geometry is that it can be produced simply by additive manufacturing, without the need for additional supports, and has a good ratio between thermal and hydraulic performance [10]. The external dimensions of the unit

cell geometry are 10 mm x 10 mm x 10 mm, and its porosity is 0.8. The equations governing continuity, momentum and energy in the fluid domain are solved. The pressure-velocity coupling is implemented by a coupled algorithm that ensures stable convergence in this case. The study is conducted in three dimensions, under equilibrium conditions, and several assumptions are made: constant thermophysical properties, incompressible and single-phase flow, steady-state flow and absence of gravity effect. This choice is justified by the fact that in the temperature range of this study (20-45 °C with the lattice structure), the specific heat, the thermal conductivity and the density varies by 0.1 %, 5 %, 1 % respectively. Although the kinematic viscosity varies by about 50 %, temperature dependent simulations showed that it had little effect on the thermal performances of the heat exchanger.

The numerical domain and boundary conditions are described in Figure 3. The upper part representing the tooling skin and lower part of the tooling are made of stainless steel, while the lattice structure is made of high-temperature thermosetting resin or stainless steel in order to study the influence of its thermal conductivity. Material properties are described in Table 1, and due to the strong thermodependency of oil (LAUDA Ultra 350) properties, its properties are described as a function of temperature (in K) in Table 2 and Table 3. A constant heat flux of 250 kW.m^{-2} is applied to the tooling surface, representing the average heat supplied by a composite part during its cooling. The fluid inlet velocity is 1 m.s^{-1}, and the fluid temperature is 20°C. To ensure hydrodynamic flow, a 100 mm long extended inlet is included. In addition, to avoid convergence problems caused by back pressure, an extended outlet section is implemented, and a relative pressure of 0 Pa is applied to the outlet boundary.

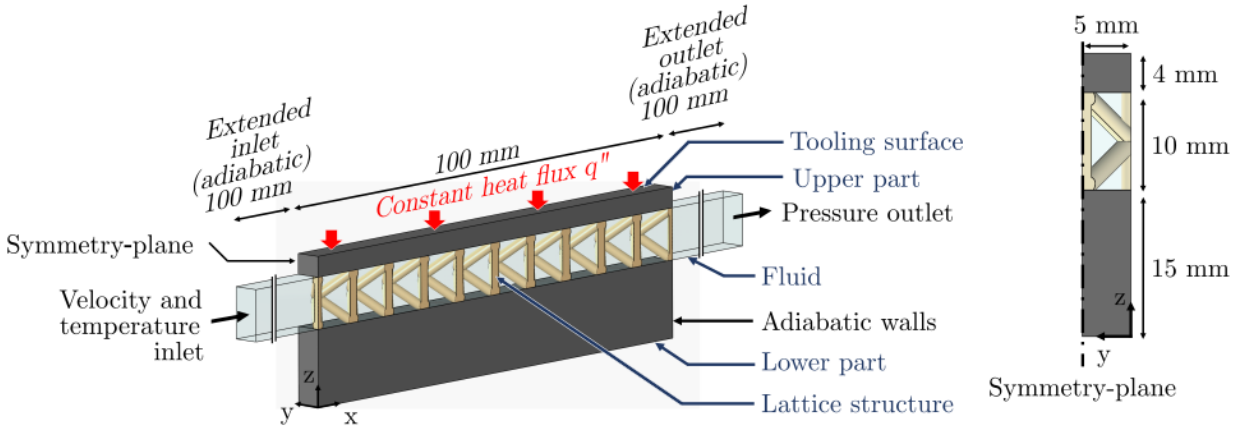

Figure 3: numerical domain and boundary conditions

A no-slip condition is applied at the fluid-solid interface. Taking advantage of the symmetry of lattice samples, only half of the configuration is simulated. The solver used is ANSYS Fluent©, and the turbulence model employed is SST k-ω, commonly used for heat transfer/fluid mechanics coupling in porous media. The model has been validated experimentally, but the validation is not presented in this paper. Simulation convergence is considered achieved when the residual values of each conserved variable are less than 10^{-4} for continuity, x-velocity, y-velocity, z-velocity, turbulent kinetic energy, turbulent dissipation rate, and 10^{-6} for energy.

Material	ρ ($kg.m^{-3}$)	λ ($W.m^{-1}.K^{-1}$)	Cp ($J.kg^{-1}.K^{-1}$)	μ ($kg.m^{-1}.s^{-1}$)
Water	998	0.60	4 182	0.001
Stainless steel	8 030	16.30	502	-
Thermoset resin	1 400	0.22	1 200	-

Table 1. Material properties

Material	μ (Pa.s)
[293.15 − 333.15]	$1.833917.10^{-8}.T^4-2.375614.10^{-5}.T^3+0.01154959.T^2-2.498098.T+202.8675$
[333.15 − 383.15]	$4.01042.10^{-10}.T^4-5.994943.10^{-7}.T^3+0.0003369473.T^2-0.08445126.T+7.9727$
[383.15 − 633.15]	$2.210252.10^{-12}.T^4-4.824272.10^{-9}.T^3+3.945593.10^{-6}.T^2-0.00143711.T+0.1977491$

Table 2. LAUDA Ultra 350 oil viscosity

Property	Value
Cp ($J.kg^{-1}.K^{-1}$)	3.69.T + 471.53
ρ ($kg.m^{-3}$)	−0.72.T + 1258.30
k ($W.m^{-1}.K^{-1}$)	−0.00013.T + 0.17

Table 3. LAUDA Ultra 350 oil properties

Experimental method.

The aim of the experimental set-up is to reproduce an industrial case with heating and cooling cycles, and to visualize the temperature at the tooling surface during the cycles to demonstrate the improvement provided by lattice structures. An experimental section representing half of the lower part of the tool is developed. The test section described in Figure 4 contains a channel through which a fluid (water) flows, with or without a lattice structure, in order to compare the two cases. Heating and cooling cycles are achieved by circulating hot and cold water in the channel. Above the channel is a stainless steel plate of 5 *mm* thickness representing the tool skin. The upper surface of this plate represents the tool surface and is visualized by the infrared camera during cycles using a FLIR X85. The camera is sensitive in the wavelength range between 1.5 µm and 5 µm with a resolution of 640×512 pixels, a maximum acquisition frequency of 1,000 Hz and a stated accuracy of ± 2°C.

The visualized surface is covered with a black paint with an emissivity of 0.87. The lower part in polycarbonate, and the lattice structure is printed in high-temperature thermosetting resin. The fluid loop shown in Figure 5 enables heating and cooling cycles to be performed by alternating cold and hot water in the test section via solenoid valves (SV). Cycles last 90 seconds, and water flow is controlled by pumps and observed by flowmeters. Temperature and pressure are acquired by thermocouples and pressure sensors at the inlet and outlet of the test section.

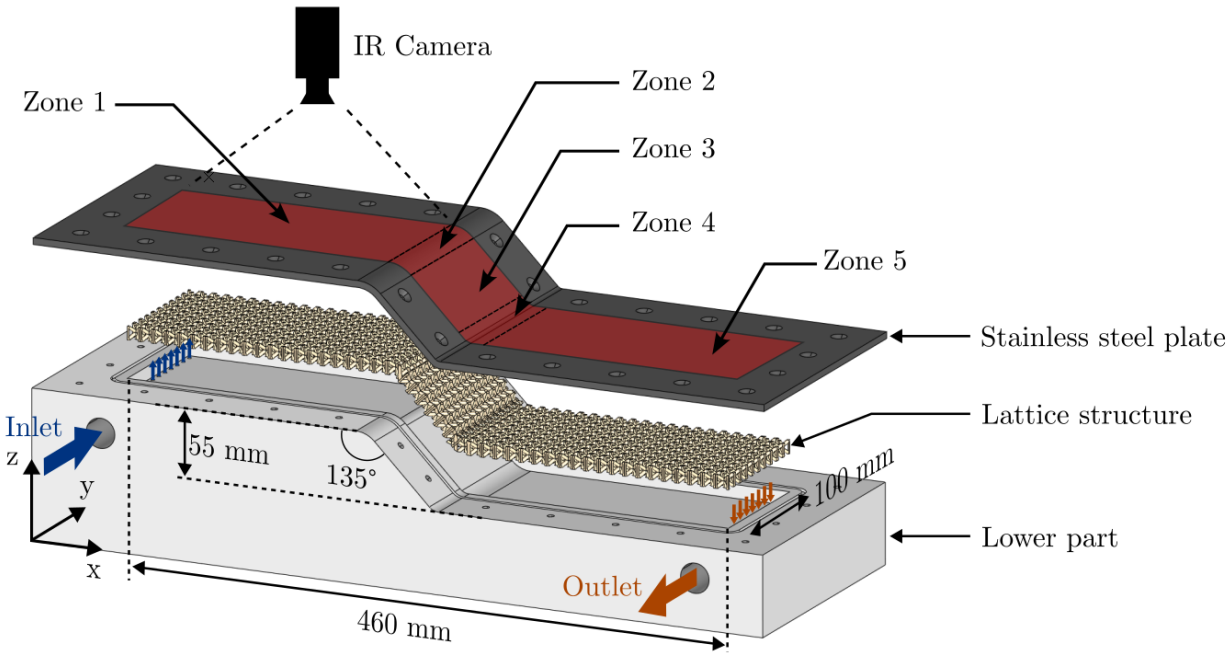

Figure 4: experimental test section

The acquisition window is divided into several zones: 1, 2, 3, 4 and 5 (as described in Figure 4), in order to achieve reasonable resolution. The test section is positioned on a system able to move it along the x-axis or rotate it along the y-axis. This ensures that the flat surfaces of zones 1, 3 and 5 are aligned perpendicular to the camera. As for zones 2 and 4, which are not flat, the system aligns their bisectors so that they are perpendicular to the camera lens. The images of the zones are then stitched together in post-processing.

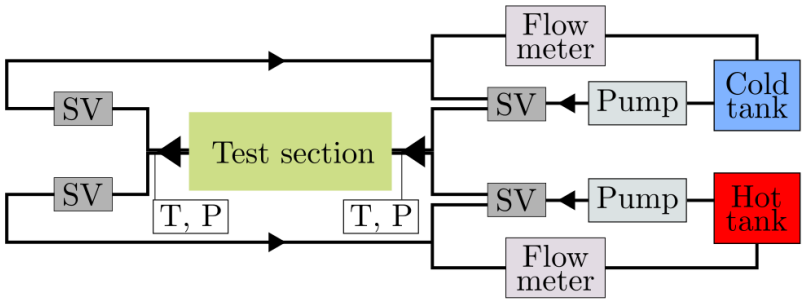

Figure 5: experimental fluid loop

Results

Steady numerical results

In the system studied, heat transfer can occur by convection between the fluid and the tool skin, or by fin effect with the heat flux conducted into the lattice and dissipated by the fluid. The heat flux

removed by the fin effect in relation to the total heat flux applied is denoted as η and defined in eq. 1.

$$\eta = {\Phi_{fin}}\Big/{\Phi_{tot}} \quad (1)$$

The heat transfer coefficient h_{eq} is defined in eq. 2

$$h_{eq} = \frac{q"}{T_{avg,tooling,skin} - T_{avg,fluid}} \quad (2)$$

With q" the applied heat flux density, $T_{avg,tooling,skin}$ the average temperature of the lower surface of the upper part (fluid/solid contact plus upper part/lattice structure contact) and $T_{avg,fluid}$ the average temperature in the fluid domain. The water average temperature increases by about 6 °C and the oil average temperature by about 16°C over this length of heat exchanger. We chose this equivalent heat transfer coefficient to compare the thermal performances of different configurations and have a global understanding of the phenomenon. The dependence of η versus the two heat transfer fluids and the lattice structure materials are presented in table 4. The contact surface area between the lattice structure and the tooling skin represents 9.1% of the total exchange surface area of the tooling skin for a porosity of the lattice structure of 0.8. Table 4 shows that the fin efficiency percentages are higher than the contact surface ratio for stainless steel lattice structure only. This result was expected as the fin efficiency depends on the ratio of the thermal resistance of the fin to the thermal resistance of the fluid. Therefore, even for laminar flow, with oil, the thermal resistance of the polymer structure is much higher than the fluid convective thermal resistance. When the flow is turbulent, with water, the thermal resistance of the fluid is lower compared to laminar flow, with oil. In consequence, the fin efficiency decreases significantly. When the thermal resistance in fin is high, such with polymer structure, the fin efficiency percentages are below the surface contact ratio value whatever the heat transfer regime studied.

	η polymer lattice structure	η stainless steel lattice structure	h_{eq} polymer lattice structure $W.m^{-2}.K^{-1}$	h_{eq} stainless steel lattice structure $W.m^{-2}.K^{-1}$	h_{eq} empty channel $W.m^{-2}.K^{-1}$
Water	0,5 %	9,8 %	14 018	16 265	5 573
Oil	1,7 %	26,5 %	2 568	3 293	1 096

Table 4. Fin effect and heat transfer coefficient in function of lattice structure material and fluid

The improvement in the convective heat transfer coefficient h_{eq} compared to the empty channel for both fluids is due to the mixing of the flow by the structure as shown in Figure 6.

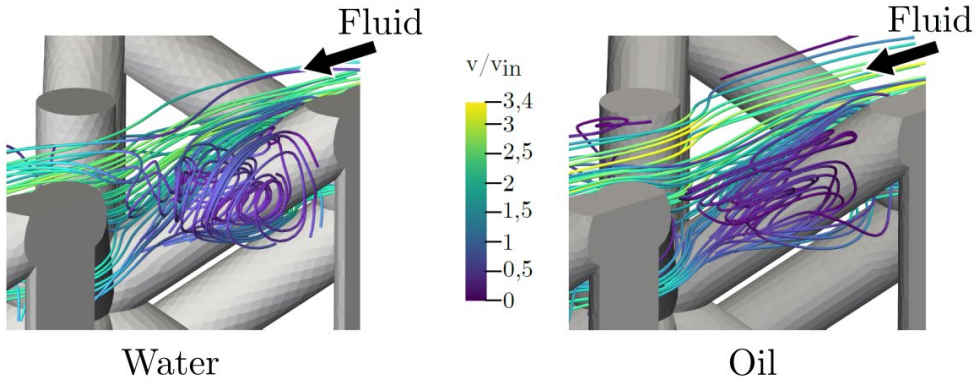

Figure 6: 3D streamlines bellow the exchange surface for water and oil

Vorticity downstream of the ligaments, flow separation and fluid acceleration are visible. The three-dimensional flow disturbance generated by the inclined lattice structure strands enhances convective exchanges, whatever the fluid: oil, with higher viscosity, or water.

Transient experimental results

In the experimental part, the transient regime is studied, in order to compare heating and cooling rates, and to analyze the uniformity of the temperature field at the tooling surface during transient phases. Only water is used as heat transfer fluid. The aim is to compare an empty channel with a channel with lattice structures. The water inlet temperature alternates between 20°C and 70°C

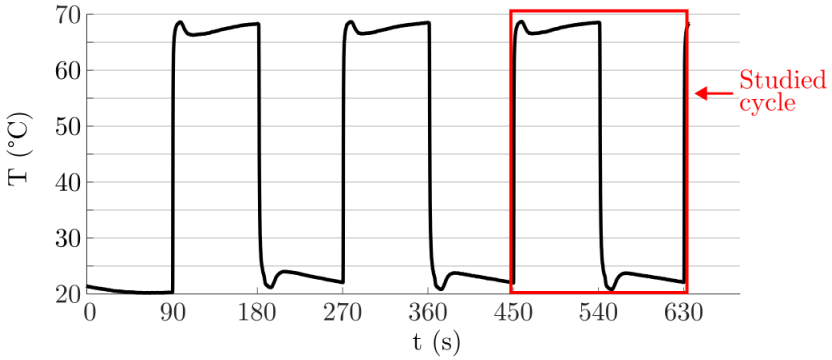

Figure 7: Temperature evolution of the fluid at the inlet of the test section

every 90 seconds, as shown in Figure 7. Slight deviations of around 4°C between set and actual temperature are observed due to the small capacity of the water tanks used for damping the fluid temperature exiting the channel to be cooled or heated. Several successive heating and cooling cycles are performed to obtain the periodic regime established on the tool surface. For the remainder of the study, a single heating/cooling cycle is used, as shown between 450 and 630 seconds in Figure 7, boxed in red.

The comparison between the empty system and the system with lattice structures is carried out at equal pumping power, with an equal product of the multiplication between mass flow rate and pressure drop, giving a mass flow rate of 4.1 $L.min^{-1}$ with the lattice structure and 6 $L.min^{-1}$ for the empty channel. The experimental temperature field at the tooling surface during the cooling phase, after 30 seconds of cooling, is shown in Figure 8. The improvement in temperature

uniformity at the tool surface during the cooling phase is clearly visible on plane surfaces and in corners.

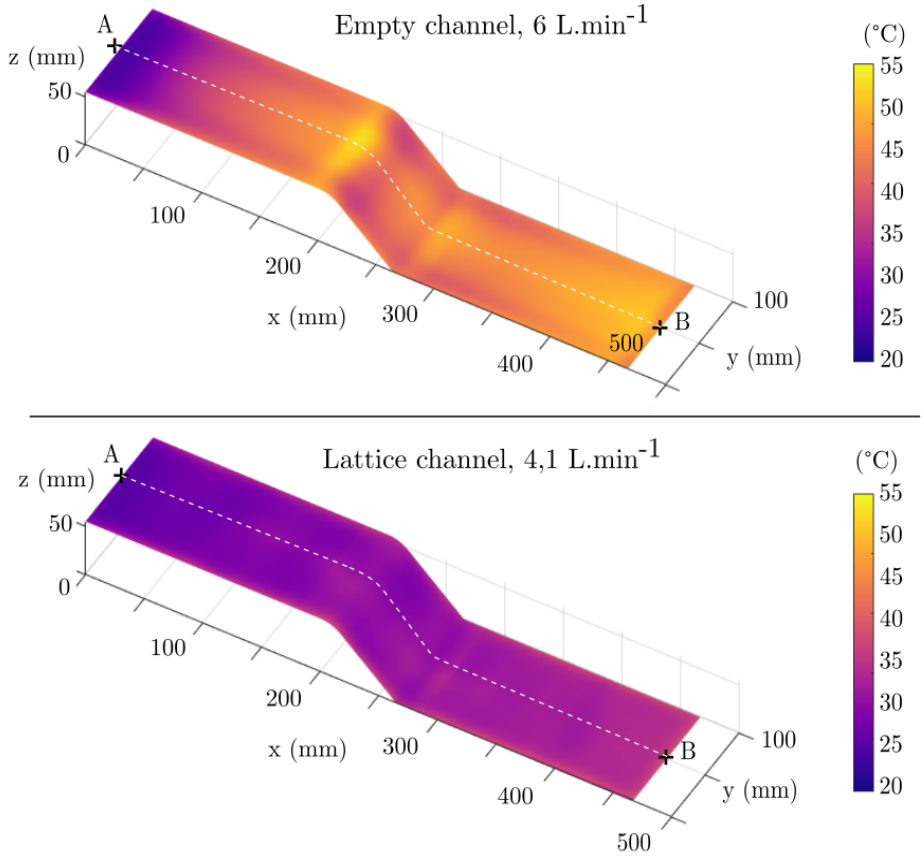

Figure 8: Experimental temperature field at tooling surface after 30 s of cooling for empty channel above and lattice channel below at equal pumping power

The temperature profile along segment [AB], dotted in Figure 9, is shown at different cooling times for the two configurations, the empty channel and the channel with lattice structures. The temperature gradient along the length of the tooling for the empty configuration throughout the cooling phase, and the impact of the corners, particularly in the convex corner, are visible. For the configuration with lattice structures, the temperature gradient is lower and the temperature is almost uniform after 45 seconds of cooling. Improved thermal management in the corners is also clearly demonstrated with lattice structures. Table 5 details the maximum temperature differences on segment [AB] during the cooling phase, confirming the improvement with lattice structures at equal pumping power.

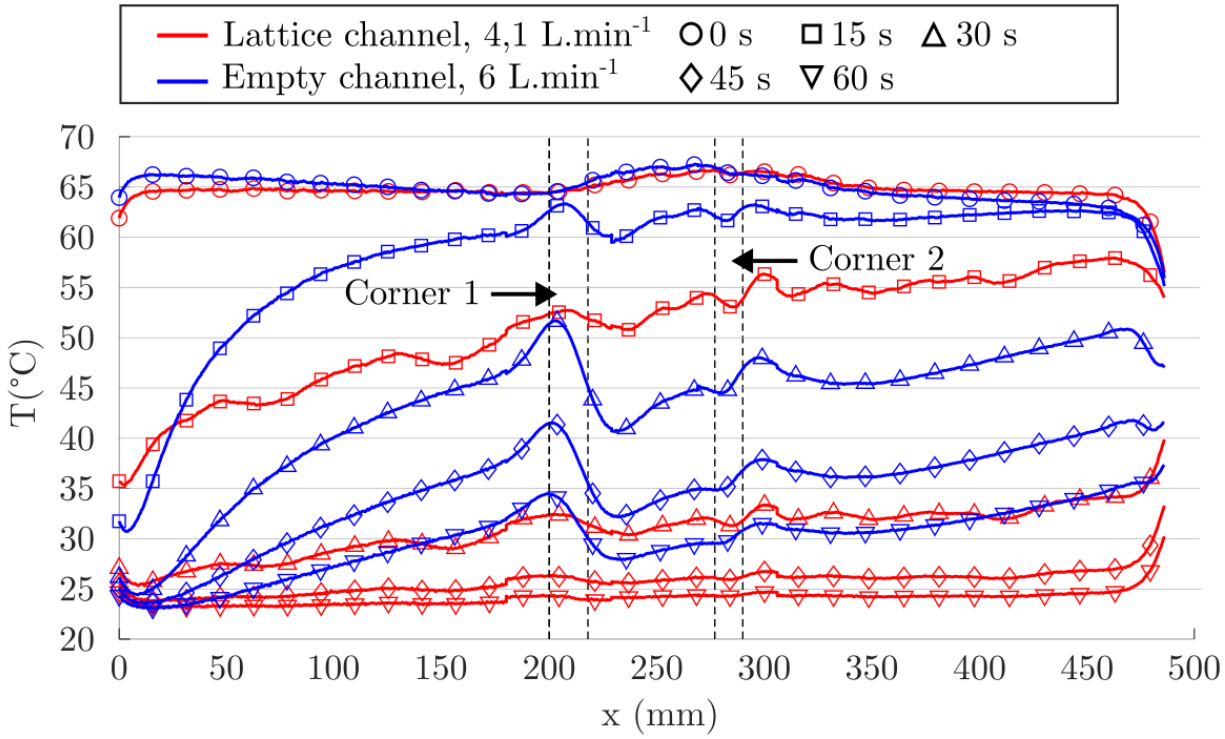

Figure 9: evolution of temperature along segment [AB] for different cooling times at equal pumping power

Cooling time	*15 s*	*30 s*	*45 s*	*60 s*
T_{max} - T_{min} lattice channel *(°C)*	22.6	14.5	9.5	7.1
T_{max} - T_{min} empty channel *(°C)*	33.0	27.9	18.7	13.9

Table 5: temperature difference between minimum and maximum value along the segment [AB] for different cooling times at equal pumping power

Conclusion

In conclusion, this article presents the advantages of lattice structures for thermal management of forming tools in composite materials. For both heat transfer fluids studied, water or oil, the lattice structure improves heat exchange, regardless of the lattice structure's thermal conductivity. In the case of oil, the heat flow evacuated by the lattice structure is greater than that of water, due to the lower convective exchange that favors the fin effect. In that case, the thermal conductivity of the lattice structure is therefore more important for the thermal performance of the tooling. For both fluids, the improvement is directly linked to the nature of the fluid flow, which is disturbed in three dimensions by the network structure favoring mixing and intense transfer near the exchange surface. In transient operation, with the same pumping power, which is an important parameter in industry, the lattice structure improves the cooling rate and uniformity over the entire tool surface in flat surfaces and tool corners.

References

[1] T. Li, Z. Song, X. Yang, J. Du, Influence of Processing Parameters on the Mechanical Properties of Peek Plates by Hot Compression Molding. Materials. 16 (2022) https://doi.org/10.3390/ma16010036

[2] T. B. Yallew, E. Kassegn, S. Aregawi, A. Gebresias. Study on effect of process parameters on tensile properties of compression molded natural fiber reinforced polymer composites. SN Appl. Sci. 338 (2020). https://doi.org/10.1007/s42452-020-2101-0

[3] P. P. Parlevliet, H. E. N. Bersee, A. Beukers. Residual stresses in thermoplastic composites - A study of the literature - Part I: Formation of residual stresses. Compos. Part Appl. Sci. Manuf. 37 (2006) 1847-1857. https://doi.org/10.1016/j.compositesa.2005.12.025

[4] S.-L. Gao, J.-K. Kim, Cooling rate influences in carbon fibre/PEEK composites. Part 1. Crystallinity and interface adhesion. Compos. Part Appl. Sci. Manuf. 31 (2000) 517-530. https://doi.org/10.1016/S1359-835X(00)00009-9

[5] A. Agazzi, V. Sobotka, R. Le Goff, Y. Jarny, Uniform Cooling and Part Warpage Reduction in Injection Molding Thanks to the Design of an Effective Cooling System. Key Eng. Mater. 554-557 (2013) 1611-1618. www.scientific.net/KEM.554-557.1611

[6] R. McCool R, A. Murphy, R. Wilson, Z. Jiang, M. Price, J. Butterfield, P. Hornsby. Thermoforming carbon fibre-reinforced thermoplastic composites. Proc. Inst. Mech. Eng. Part J. Mater. Des. Appl, 226 (2012) 91-102. https://doi.org/10.1177/1464420712437318

[7] Arman, S. and Lazoglu, I. A comprehensive review of injection mold cooling by using conformal cooling channels and thermally enhanced molds. Int J Adv Manuf Technol 127 (2023) 2035–2106. https://doi.org/10.1007/s00170-023-11593-w

[8] J. Tian, T. Kim, T.J. Lu, H.P. Hodson, D.T. Queheillalt, D.J. Sypeck, H.N.G. Wadley, The effects of topology upon fluid-flow and heat-transfer within cellular copper structures, International Journal of Heat and Mass Transfer, 47 (2004) 3171-3186, https://doi.org/10.1016/j.ijheatmasstransfer.2004.02.010

[9] M. F. Ashby, The Properties of Foams and Lattices. Philosophical Transactions: Mathematical, Physical and Engineering Sciences, 364 (2006) 15–30, http://www.jstor.org/stable/25190170

[10] M. Balthazar, N. Baudin, J. Soto, D. Edelin, S. Guéroult, V. Sobotka, Improvement of thermal management of composites forming process tooling using lattice structures. Int J Adv Manuf Technol 134 (2024) 2705–2723. https://doi.org/10.1007/s00170-024-14264-6